Importance of the Solvent-Exposed Residues of the Insulin B Chain α-Helix for Receptor Binding[†]

Tine Glendorf,* Anders R. Sørensen, Erica Nishimura, Ingrid Pettersson, and Thomas Kjeldsen

Diabetes Protein Engineering, Novo Nordisk A/S, Novo Nordisk Park, DK-2760 Måløv, Denmark

Received January 10, 2008; Revised Manuscript Received March 5, 2008

ABSTRACT: Conjointly, the solvent-exposed residues of the central α-helix of the B chain form a well-defined ridge, which is flanked and partly overlapped by the two described insulin receptor binding surfaces on either side of the insulin molecule. To evaluate the importance of this interface in insulin receptor binding, we developed a new powerful method that allows us to introduce all the naturally occurring amino acids into a given position and subsequently determine the receptor binding affinities of the resulting insulin analogues. The total amino acid scanning mutagenesis was performed at positions B9, B10, B12, B13, B16, and B17, and the vast majority of the insulin analogue precursors were expressed and secreted in amounts close to that of the wild-type (human insulin) precursor. The analogue binding data revealed that positions B12 and B16 were the two positions most affected by the amino acid substitutions. Interestingly, the receptor binding affinities of the B13 analogues were also markedly affected by the amino acid substitutions, suggesting that GluB13 indeed is a part of insulin's binding surface. The B10 library screen generated analogues covering a wide range of (20–340%) of relative binding affinities, and the results indicated that a structural stabilization of the central α-helix and thereby a more rigid presentation of the binding epitope at the insulin receptor is important for receptor recognition. In conclusion, systematic amino acid scanning mutagenesis allowed us to confirm the importance of the B chain α-helix as a central recognition element serving as a linker of a continual binding surface.

Insulin is a small globular protein consisting of an A chain of 21 amino acids and a B chain of 30 amino acids. The two chains are covalently linked by disulfide bridges directing the A chain to be positioned with its two α-helices resting on the central α-helix of the B chain (*1*). Insulin elicits its biological response through the insulin receptor (IR),[1] a covalent dimer consisting of two extracellular α-subunits and two transmembrane β-subunits and found in two isoforms, which differ in the absence [A-isoform (IR-A)] or presence [B-isoform (IR-B)] of a 12-amino acid sequence at the C-terminal end of the insulin-binding α-subunit. The two isoforms are generated as a result of alternative splicing of the insulin receptor gene; however, the exact physiological significance of this phenomenon, which is tissue-specific, remains incompletely understood (*2*). Even though the molecular structures of insulin and its receptor have been subjected to elaborate investigations for many years (*3–9*) and the crystal structure of the IR ectodomain recently has been determined (*10*), a detailed structure of the insulin−receptor complex has not yet been obtained. Consequently, the exact mechanism of insulin binding and mapping of the entire insulin binding surface involved herein remain to be fully elucidated.

Nevertheless, analysis of receptor binding properties and structures of insulin analogues and comparisons of sequences and binding properties of insulin from different animal species (*4, 6, 11–13*) have resulted in the consensus being that the so-called "classical binding surface" is made up of residues A1, A5, A19, A21, B12, B16, and B23−B26, which partly overlap with the dimer-forming surface, together with nonsurface residues A2 and A3 (*14, 15*) believed to be exposed upon receptor binding (*16–22*) (see Figure 1b). On the basis of studies of insulin analogues with aberrant binding properties similar to those of hagfish (*23, 24*) and hystricomorph insulin (*25, 26*), a second binding surface comprising residues A13 and B17 located in the hexamer-forming surface on the opposite side of the molecule was later proposed (*27, 28*). The existence of a second binding surface allowing insulin to contact both monomers in the IR dimer provides a plausible explanation for the negative cooperativity and curvilinear Scathard plots observed in IR binding studies (*29*) and is supported in a model based on the newly determined structure of the IR ectodomain (*30, 31*).

The two currently described binding surfaces on either side of the molecule are separated by the central α-helix of the B chain. The solvent-exposed residues of the α-helix

[†] This work was supported by the Danish Ministry of Science, Technology and Innovation and the Novo Nordisk CORA Training and Research Program.

* To whom correspondence should be addressed. E-mail: tgle@novonordisk.com. Telephone: (+45) 44436277. Fax: (+45) 44444256.

[1] Abbreviations: ALP, *Achromobacter lyticus* protease; BHK, baby hamster kidney; BSA, bovine serum albumin; CD, circular dichroism; DKP-insulin, monomeric insulin analogue containing three B chain substitutions (B10D, B27K, and B28P); HI, human insulin; IR, insulin receptor; IR-A, A-isoform of the IR without exon 11; IR-B, B-isoform of the IR with exon 11; MALDI-TOF, matrix-assisted laser desorption ionization time-of-flight; MS, mass spectrometry; RP-HPLC, reverse-phase high-performance liquid chromatography; SPA, scintillation proximity assay; TFA, trifluoroacetic acid. Amino acid residues occurring in human insulin in a given position are designated by three-letter codes, whereas introduced amino acid substitutions are designated by one-letter codes.

10.1021/bi800054z CCC: $40.75
Published on Web 04/01/2008

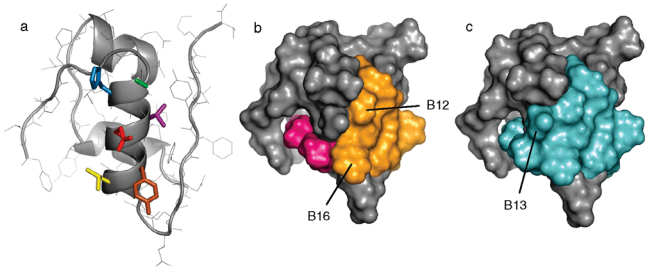

FIGURE 1: Structure of the insulin molecule. (a) Ribbon representation of insulin in which the side chains of the solvent-exposed residues (B9, green; B10, blue; B12, purple; B13, red; B16, brown; B17, yellow) on the central α-helix of the B chain are highlighted. (b) Surface representation of insulin, in which residues of the two currently described binding surfaces are highlighted. Residues of the classical binding surface are colored orange (A1−A3, A5, A19, A21, B12, B16, and B23−B26), while residues of the second putative binding surface are colored pink (A13 and B17). (c) Surface representation of insulin with the continual binding surface (A1−A3, A5, A19, A21, B12, B13, B16, and B23−B26) colored light blue. Orientations of the molecules are identical in all three panels. Coordinates for the structure of insulin in the T conformation (Protein Data Bank entry 1MSO) (*64*) were obtained from the Protein Data Bank and visualized using PyMOL (*65*).

comprising SerB9, HisB10, ValB12, GluB13, TyrB16, and LeuB17 form a well-defined surface on the insulin molecule, which borders and partially overlaps the two binding surfaces (see Figure 1) and was therefore hypothesized to play a principal role in receptor binding. To evaluate this hypothesis, we have developed a new powerful method that facilitates total amino acid scanning mutagenesis on the different positions of the insulin molecule.

A number of analogues with mutations in the solvent-exposed residues on the central α-helix of the B chain have previously been reported (*13, 32–35*). However, in this study, a more comprehensive structure–function analysis was undertaken by systematically introducing the 20 naturally occurring amino acids at each of the solvent-exposed positions of insulin's central α-helix. All the insulin analogues were individually evaluated in terms of IR affinity, and the results underline the importance of residues ValB12, GluB13, and TyrB16 in insulin−receptor interactions.

EXPERIMENTAL PROCEDURES

Miscellaneous. Human insulin, [^{125}I]TyrA14-labeled insulin, and immobilized *Achromobacter lyticus* protease (ALP) were from Novo Nordisk A/S. Binding assays were performed using IR-specific monoclonal mouse antibody 83-7 (*36*) licensed from K. Siddle (University of Cambridge, Cambridge, U.K.) and solubilized human IR (holoreceptor) semipurified by WGA purification (according to the method from ref *37*) from baby hamster kidney (BHK) cells, which were stably transfected with the pZem vector containing either the human IR-A or IR-B insert (*38*). Chemicals used were of analytical grade or higher from Sigma-Aldrich.

Total Amino Acid Scanning Mutagenesis. (i) Vector Construction and Precursor Expression in Yeast. Materials, strains, general molecular biology techniques, and the yeast expression system were as previously published unless otherwise mentioned (*13, 39, 40*). Mutations were inserted into the sequence encoding the insulin precursor by overlap extension PCR (*41*) using appropriate primers with mixed oligonucleotides in the desired codons. The insulin precursors were expressed as proinsulin-like fusion proteins, with an Ala-Ala-Lys mini C-peptide (*42*) in *Saccharomyces cerevisiae* strain MT663, and transformed and selected as previously described (*13*). Insulin precursor fermentation yields were quantified by reverse-phase high-performance liquid chromatography (RP-HPLC) using human insulin as an external standard.

(ii) Enzymatic Conversion of Insulin Precursors. The single-chain precursors were enzymatically converted into two-chain desB30[2] analogues using the lysine-specific *A. lyticus* endoprotease, which causes an approximate 35% decrease in analogue concentration that can be attributed to dilution as well as removal of the extension and the mini C-peptide. Clarified supernatants containing the insulin precursors were treated with ALP immobilized on Sepharose at pH 8 (*13*). The matrix-bound protease was removed by centrifugation. Concentrations of the desB30 insulin analogues were determined by RP-HPLC using human insulin as an external standard. The efficiency of the conversion of the insulin precursors into the corresponding desB30 insulin analogues was readily evaluated given that the removal of the extension and mini C-peptide has a significant impact on the retention time of the molecule in analytical RP-HPLC. All amino acid substitutions and full conversion of the precursors were confirmed by matrix-assisted laser desorption ionization time-of-flight (MALDI-TOF) mass spectrometry (MS).

(iii) Insulin Receptor Binding Assay. Competition binding assays were conducted on an Eppendorf epMotion 5075 robot in 96-well plates (polystyrene Optiplate-96, PerkinElmer). Assays were initiated by making dilution series (eight dilutions, 5-fold each, first dilution 43-fold) of the yeast supernatant containing the insulin analogue ($n = 4$ on each plate) and human insulin ($n = 4$ on each plate) in binding buffer followed by addition of a premixed mixture of scintillation proximity assay (SPA) beads (SPA PVT Antibody-Binding Beads, Anti-Mouse Reagent, GE Healthcare) resuspended in binding buffer, anti-IR mouse antibody (83-7), solubilized human IR (IR-A or IR-B), and [^{125}I]TyrA14-labeled insulin. The final concentration of [^{125}I]TyrA14-labeled insulin was 7.5 pM, and the buffer consisted of 100 mM HEPES (pH 7.8), 100 mM NaCl, 10 mM $MgSO_4$, 0.025% (v/v) Tween 20, and 0.5% (w/v) BSA (A-7888). Plates were incubated with gentle shaking for 24 h at room temperature, centrifuged, and counted in a TopCounter (PerkinElmer) for 3 min/well. The percentage of tracer bound in the absence of competing ligand was less than 15% in all assays, to prevent ligand-depletion artifacts. A wild-type insulin precursor converted to two-chain desB30 human insulin in yeast supernatant was included as an internal control for each library analysis that was performed. None of the analogues containing Lys or Cys substitutions were included in the SPA due to probable ALP cleavage in the conversion step or potential disulfide mispairing, respectively. Data from the SPA were analyzed according to the four-parameter logistic model (*43*) assuming constant slope, basal, and maximal response. The affinities (picomolar affinity range) of the analogues are expressed relative to that of human insulin [IC_{50}(insulin)/IC_{50}(analogue) × 100%] measured within the same plate.

[2] Insulin lacking the amino acid at position B30.

(iv) Purification of Selected Analogues. To validate the use of insulin analogues directly in the yeast supernatant in the SPA, a selection of analogue strains was fermented to yield between 0.9 and 3.4 L of fermentation culture. The secreted analogue precursors (B10R, B10N, B10Q, B10E, B10H, B10I, B10F, B10W, and B10V) were enzymatically cleaved into two-chain insulin analogues and purified according to the standard procedure (*42*). Briefly, the insulin precursor was captured from cell-free acidified culture supernatant on a cation exchange column. The eluted precursor was processed by immobilized ALP and further purified by preparative RP-HPLC, from which the main protein peak was collected and lyophilized. Full conversion to the two-chain desB30 analogue was verified by MALDI-TOF MS, and the purity was measured by RP-HPLC at both acidic and neutral pH.

RESULTS

Analogue Construction and Expression in Yeast. Conjointly, the solvent-exposed residues of the central α-helix of the B chain form a protruding ridge, which partly converges with the two flanking binding surfaces of insulin. Given its location, we decided to address the importance of this interface in IR binding. We developed a new powerful method, which enabled us to introduce all the naturally occurring amino acids at positions B9, B10, B12, B13, B16, and B17 and subsequently evaluate the receptor binding affinities of the 120 resulting insulin analogues (including the six desB30 human insulin internal controls).

The insulin precursors were individually expressed in *S. cerevisiae* and fermented in 5 mL cultures, and the yield of the secreted precursor was determined by RP-HPLC. The vast majority of the insulin analogue precursors were expressed in amounts close to that of the wild-type precursor, and in fact, 30% of the analogues were expressed and secreted in amounts exceeding that of the wild-type precursor, indicating correct processing and folding of the precursors in the yeast cell (*44*). The highest expression levels were obtained in the B9 library, while amino acid substitutions in the B12 position had the most deleterious effects on expression yields, suggesting that the substitutions at B12 induce structural changes affecting efficient precursor folding. As expected, most of the precursors containing Cys and Pro substitutions were poorly expressed or expressed in undetectable amounts, and except for these two substitutions, only four precursors in which the invariant ValB12 residue was replaced with either Asn, Gly, His, or Ser were expressed in amounts that were less than 5% of that of the wild-type precursor. In the remaining libraries, the lowest expression yields were between 20 and 42% compared to that of the wild-type precursor.

Insulin Receptor Binding. Following enzymatic conversion, the receptor affinities of the two-chain desB30 insulin analogues were determined by SPA in 96-well formats using human IRs purified from BHK cells (see Table 1 and Figures 2 and 3). For each analogue, assays were performed on both the A- and B-isoforms of the IR, the two serving as duplicate assays since the correlations between the relative affinities determined on the two receptor isoforms were very high for all six analogue libraries. To verify the reproducibility of the assay, 10 of the analogues in yeast supernatant were further tested in at least three independent experiments on both isoforms of the IR and the average relative binding potencies with standard deviations are listed in Table 1. For these 10 analogues, the differences between the average relative binding potencies determined on either receptor isoform were not found to be statistically significant, while the small differences between the IR-A and IR-B binding potencies for the analogues tested once most likely were attributable to assay variation.

The binding experiments were conducted on an Eppendorf robot allowing consistent and expeditious determination of receptor binding affinities for a large number of analogues. For each plate, a purified insulin standard and one insulin analogue were applied and displacement of ^{125}I-labeled insulin was assessed. The resulting average relative binding affinities of the internal desB30 insulin controls were 98 and 4% when tested on either isoform of the IR ($n = 10$ and $n = 9$ for the A- and B-isoforms, respectively), thus validating the use of insulin analogues directly in supernatant for the competitive binding experiments. Examples of competition binding curves are given in Figure 2.

To further affirm the validity of using insulin analogues directly in yeast supernatant in the IR binding experiments, a selection of 10 *S. cerevisiae* strains was fermented and the secreted insulin analogue precursors were enzymatically cleaved and purified (97.2–99.9% pure). The relative binding affinities of these purified analogues were subsequently measured in the SPA in at least three independent experiments on both isoforms of the IR, and a strong correlation ($R^2 = 0.97$) between the relative affinities measured on purified analogues and analogues in yeast supernatant was observed (see Figure 4).

The systematic amino acid scanning mutagenesis identified position B13 to be markedly affected by the introduced amino acid substitutions. Only the conservative substitution of B13Glu with Asp or replacement of Glu with Trp resulted in analogues with almost fully retained receptor affinities, while 2-fold[3] reductions in receptor affinities were observed for B13I and B13M. The residual B13 analogues exhibited more pronounced decreases in the level of receptor binding. In fact, amino acid substitution of GluB13 had a greater impact on receptor binding affinities than the mutations at LeuB17. LeuB17 is featured in the second putative binding site of the insulin molecule; however, this position was surprisingly mildly affected by the introduced amino acid substitutions. Analogues B17M, B17F, and B17W exhibited almost fully preserved binding affinities, while all the remaining analogues except B17R (6-fold reduction) merely displayed 2–3-fold reductions in binding affinities.

Interestingly, the amino acid substitutions at position B10 generated analogues covering a wide range (20–340%) of relative binding affinities. As expected from earlier studies (*32, 45*), both of the negatively charged substitutions to either Asp or Glu led to an approximate 3-fold increase in IR affinity, while analogues B10Q, B10I, B10M, and B10F exhibited a more moderate increase in binding affinities. Surprisingly, B10 was the only position in which the introduced amino acid substitutions resulted in analogues with significantly increased receptor affinities.

[3] The relative binding affinities mentioned in the text are averages of the relative binding affinites measured on IR-A and IR-B.

Table 1: Insulin Analogue Receptor Binding Data (% of human insulin)[a]

insulin analogue		A-isoform of the IR	B-isoform of the IR	insulin analogue		A-isoform of the IR	B-isoform of the IR
B9	A	51	61	B13	A	18	14
B9	R	24	28	B13	R	8	9
B9	N	21	23	B13	N	29	28
B9	D	8	12	B13	D	88	91
B9	Q	17	18	B13	Q	18	17
B9	E	13	16	B13	E	101	95
B9	G	53	52	B13	G	16	15
B9	H	41	52	B13	H	26	27
B9	I	9	10	B13	I	47	56
B9	L	9	9	B13	L	19	26
B9	M	21	23	B13	M	43	49
B9	F	99	106	B13	F	20	20
B9	P	39	35	B13	P	NE[b]	NE[b]
B9	S	98	94	B13	S	15	19
B9	T	31	27	B13	T	24	23
B9	W	105	112	B13	W	94	94
B9	Y	83	74	B13	Y	35	31
B9	V	15	14	B13	V	38	43
B10	A	39 ± 4	44 ± 4	B16	A	30	32
B10	R	18 ± 4	21 ± 1	B16	R	7	8
B10	N	76	64	B16	N	15	14
B10	D	270 ± 37	275 ± 6	B16	D	4	4
B10	Q	121 ± 4	120 ± 5	B16	Q	9	10
B10	E	340 ± 26	339 ± 8	B16	E	4	4
B10	G	37	36	B16	G	4	5
B10	H	101 ± 5	99 ± 6	B16	H	20	25
B10	I	140 ± 40	140 ± 36	B16	I	22	23
B10	L	96	90	B16	L	24	30
B10	M	158	145	B16	M	15	13
B10	F	134 ± 6	133 ± 4	B16	F	84	95
B10	P	76	76	B16	P	NE[b]	NE[b]
B10	S	44	40	B16	S	9	10
B10	T	42	41	B16	T	2	2
B10	W	89 ± 13	91 ± 3	B16	W	92	100
B10	Y	69	51	B16	Y	97	96
B10	V	81 ± 8	95 ± 11	B16	V	24	25
B12	A	1	2	B17	A	33	36
B12	R	≤0.1	≤0.1	B17	R	15	16
B12	N	≤0.1	≤0.1	B17	N	24	24
B12	D	≤0.1	≤0.1	B17	D	29	33
B12	Q	≤0.1	≤0.1	B17	Q	25	28
B12	E	≤0.1	≤0.1	B17	E	30	30
B12	G	≤0.1	0.3	B17	G	25	25
B12	H	0.2	0.2	B17	H	33	30
B12	I	16	17	B17	I	47	52
B12	L	4	5	B17	L	92	96
B12	M	3	4	B17	M	86	98
B12	F	0.2	0.3	B17	F	74	73
B12	P	4	5	B17	P	NE[b]	NE[b]
B12	S	0.5	0.6	B17	S	34	36
B12	T	6	8	B17	T	39	32
B12	W	≤0.1	≤0.1	B17	W	86	94
B12	Y	≤0.1	≤0.1	B17	Y	45	37
B12	V	97	100	B17	V	42	38

[a] For analogues tested in at least three independent experiments, averages of the relative binding potencies ± the standard deviation are presented. [b] Not expressed in *S. cerevisiae*.

The importance of positions B12 and B16 in IR binding was confirmed by the amino acid scanning mutagenesis. Both positions are part of the classical binding surface and were also the two positions which were most affected by amino acid substitutions with regard to receptor binding. Replacement of the invariant valine residue in position B12 was the most disruptive of binding. In this insulin analogue library, B12I was the analogue with the highest expression yield (74% of that of the wild type) and at the same time the analogue displaying the highest relative binding affinity (17%). The rest of the amino acid substitutions at B12 were even more disruptive with respect to binding, and only the four analogues B12L (4%), B12M (4%), B12P (4%), and B12T (7%) exhibited relative binding affinities of ≥1% compared to human insulin.

In human insulin, position B16 is occupied by a tyrosine residue and only conservative amino acid substitutions to either Phe or Trp were well tolerated and resulted in binding potencies close to that of insulin. Substitution with some of the smaller hydrophobic amino acids such as Ala, Ile, Leu, and Val but also His caused a moderate 3–4-fold reduction in binding affinity, whereas the remaining amino acid substitutions at this position had a much greater impact on receptor binding. The most affected analogue in the B16 library was analogue B16T, which retained only 2% of the binding affinity of human insulin. Less detrimental reductions

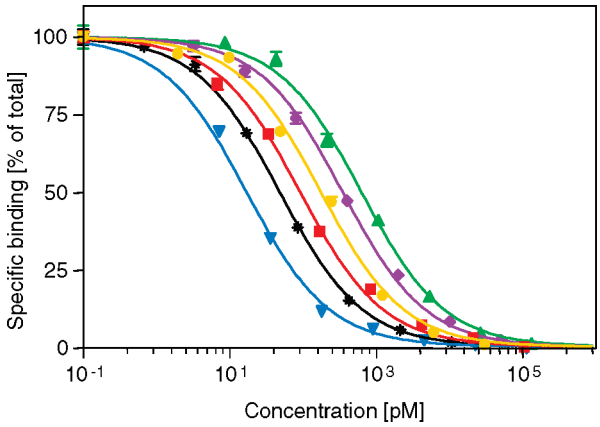

FIGURE 2: Competition curves for displacement of ^{125}I-labeled insulin by insulin and insulin analogues from the IR. The graphs are representatives of competition curves obtained from the SPA with soluble IR-A as described in Experimental Procedures. The amount of bound ^{125}I-labeled insulin as a percentage of bound ^{125}I-labeled insulin in the absence of an unlabeled insulin analogue is plotted against the concentration of unlabeled insulin analogue. Each assay point on the graphs is the mean ± the standard deviation of four measurements within one assay ($n = 1$). The ^{125}I-labeled insulin was displaced with purified human insulin (*) or insulin analogues (unpurified) B9I (▲), B10E (▼), B12 (◆), B13M (■), and B17G (●) expressed in yeast supernatant and converted by ALP treatment.

in binding affinities were observed when TyrB16 was replaced with Asn or Gln, which resulted in 7- and 11-fold reductions, respectively. However, exchanging the amide groups of B16N and B16Q with carboxylate groups prompted 25-fold reductions in binding affinities for both the B16D and B16E analogues.

The B9 position at the N-terminus of the central α-helix was less significantly affected by the amino acid substitutions. Analogues with both small hydrophilic and large hydrophobic side chains were able to make adequate contacts with the IR. Especially mutations to the aromatic amino acids were very tolerated well with respect to binding, while analogues B9A, B9G, B9H, B9P, and B9T exhibited only 2–3-fold reductions in binding affinity compared to human insulin. The rest of the substitutions were more disruptive of binding (up to 11-fold reductions).

DISCUSSION

This study has focused on the importance of the solvent-exposed residues of the central α-helix of the B chain in IR binding. Jointly, these six residues form a well-defined ridge partly overlapping the two currently described binding surfaces on either side of the helix. The screening of a large number of insulin analogues was rendered possible by employing an approach in which the IR affinity of the analogues was reliably assessed directly in yeast supernatant without purification. The total amino acid scanning mutagenesis was made practicable using yeast secretory expression, semiautomation, and SPA technology and enabled identification of structural requirements of different amino acid side chains for IR binding. In total, 120 insulin analogue precursors were expressed in yeast and converted to desB30 insulin analogues by ALP treatment. The receptor binding potencies of the analogues for the A- and B-isoforms of the receptor were determined by use of purified IRs immobilized on SPA beads.

The acquired binding data confirm the importance of the B chain α-helix of insulin in receptor binding. By using human IM9 lymphocytes to evaluate the binding properties of a B13A analogue, GluB13 which is featured in the dimer-forming surface of insulin has recently been proposed to be part of the second putative binding surface (*46*). The results obtained in this study employing total amino acid scanning mutagenesis also suggested that B13 does take part in insulin−receptor interactions. In fact, amino acid substitutions at this position affected the relative binding affinity of the corresponding analogues more severely than substitutions at position B17. The involvement of GluB13 in receptor binding is also plausible given that GluB13 is situated between ValB12 and TyrB16, shown to be very important for receptor binding. Not surprisingly, the IR binding affinity was almost unaffected by the conservative Asp mutation. Interestingly though, the B13W analogue was able to bind to the IR with nearly the same affinity as human insulin. Within proteins and in protein–protein interactions, the side chains of aromatic amino acids such as Phe, Tyr, and Trp are able to make favorable cation−π interactions with the positively charged side chains of both Arg and Lys. Among the aromatics, Trp is evidently the most likely to be involved in a cation−π interaction and preferably with an Arg residue (*47*). Since cation−π interactions have been shown to play an important role in intermolecular recognition at protein–protein interfaces (*47, 48*) and since both the negatively charged Asp and the aromatic Trp residues inserted at B13 were tolerated well with regard to binding, it is therefore tempting to speculate that GluB13 makes favorable interactions with a positively charged residue(s) on the IR. Such interactions would be in good agreement with the insulin binding model of Lou et al. (*30*) in which GluB13 is able form favorable interactions with Arg118, Gln34, and Arg65 on the IR L1-binding surface.

In the β-cell, HisB10 plays an important role in hexamer formation by the coordination of zinc (*49*) and functions in processing and transport of the insulin molecule through the secretory pathway (*50*). However, as one can see from Figure 3, a histidine residue is not required for IR binding; in fact, a diverse array of amino acid side chains are allowed in this position. A number of B10 analogues have previously been reported (*32, 45, 51, 52*), including B10K, which retained 17% binding affinity. In this study, the B10K analogue was not included in the receptor assays due to probable cleavage at this position by the use of lysine-specific ALP in the precursor conversion step. Here, substitution with another positively charged amino acid, Arg, resulted in a similar 5-fold reduction in the level of receptor binding, which in fact was the most pronounced decrease in binding affinity observed in the B10 library. Inversely, analogues B10D and B10E carrying negatively charged amino acid side chain substitutions exhibited very high relative binding affinities of 273 and 340%, respectively, which are in good agreement with previous findings (*32, 45*). Analyses of α-helices from protein structures have previously shown that Asp and Glu located at the N-terminus are able to stabilize the α-helical structure by N-terminal capping (*53–55*), and introduction of either of the two amino acids at position B10 of insulin has in fact been shown to cause a substantial enhancement of both the folding stability and the biological activity of the molecule (*32*). Conversely, the positively charged side

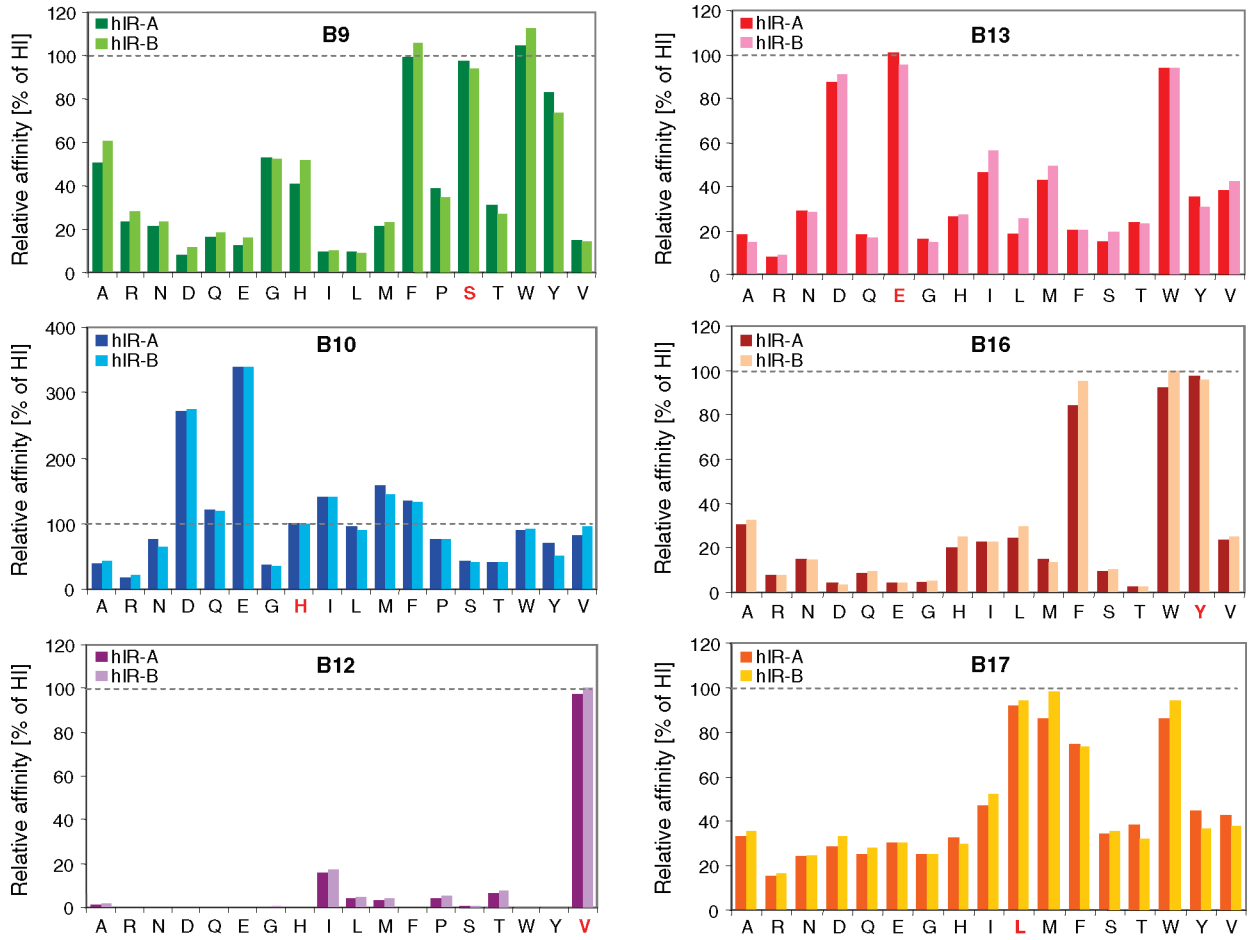

FIGURE 3: Overview of insulin analogue receptor binding data. All the data represent IR affinities relative to that of human insulin determined by competition experiments using SPA technology (see Table 1). The relative binding affinities are plotted as a function of the amino acid substitutions in the given positions. For each position, the dark-colored bars represent binding data obtained on IR-A, whereas the light-colored bars represent binding data obtained on IR-B. For each library, the amino acid representing the internal desB30 human insulin control is printed in red and the gray dotted line represents 100% binding affinity compared to that of human insulin. Relative binding affinities are calculated as the ratio of analogue to human insulin required to displace 50% of the specifically bound ^{125}I-labeled insulin.

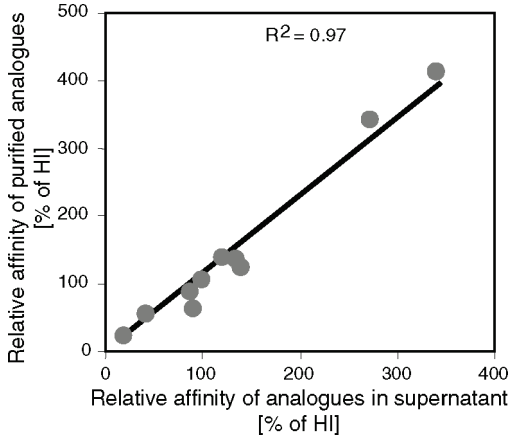

FIGURE 4: Correlation between the relative binding affinities measured on the insulin analogues (B10R, B10N, B10Q, B10E, B10H, B10I, B10F, B10W, and B10V) in yeast supernatant and the corresponding insulin analogues in purified form.

chains of the Arg and Lys residues at B10 might form unfavorable and destabilizing interactions with the helix dipole of the central α-helix, which perhaps could explain the decreases in binding affinity observed for the B10R and the B10K (*51*) analogues. Interestingly, analogues B10F, B10M, and B10I all display binding affinities higher (>130%) than that of human insulin. This observation may be explained by the possible structural stabilization of the central α-helix through hydrophobic interactions between the amino acid side chain in B10 and B6, which enhances receptor binding. In summation, though a histidine residue at B10 is inessential for receptor binding, an increase in helix stability appears to be an important factor contributing to an increased level of receptor recognition.

LeuB17 is believed to be part of the second putative binding surface (*27, 28*), which overlaps with the hexamer-forming surface on the insulin molecule. Taking this information into account, we found the amino acid substitutions at B17 had a less dramatic impact on receptor binding affinity than expected. In this study, several of the analogues with hydrophobic substitutions (B17L, B17M, B17F, and B17W) displayed binding affinities comparable to that of human insulin, while the majority of the remaining substitutions caused moderate 2–3-fold reductions in receptor binding affinity. However, the identification of a second domain on insulin important for binding was based on observations of analogues displaying anomalous receptor binding kinetics. The amino acid side chain at position B17 protrudes from the surface of the molecule, and receptor interactions are therefore plausible; however, measuring equilibrium binding alone may underestimate the impact of the mutations on the association and dissociation rates of the analogues.

Among the six positions examined in this study, the most deleterious effects of the amino acid substitutions were observed in the B12 library, with respect to both expression yields and receptor binding. The invariant valine residue at B12, which is part of the nonpolar surface involved in dimer formation, is partly exposed on the surface and partly packed against the C-terminal β-strand of the B chain within the monomer, where the B12 side chain makes favorable van der Waals interactions with the side chains of B24 and B26, which stabilize the conformation of the molecule. The binding data obtained in this study are in good agreement with previous work in which the substitution of ValB12 with either natural or unnatural amino acids has been shown to cause severe decreases in binding affinity (*35, 56–59*). As in the previous investigations of the B12 position, the most tolerated natural amino acid substitution was found to be the nonpolar Ile substitution; albeit, the resulting B12I analogue retained merely 17% of the binding affinity of human insulin. The majority of the remaining B12 analogues displayed binding potencies $\leq$1% of that of human insulin.

Huang and co-workers (*56*) have recently demonstrated that a number of B12-DKP-insulin analogues, including B12A and B12T, were structurally similar to that of the parent monomer (*60*). The significant impairments in binding affinities of these substitutions despite the absence of transmitted structural changes therefore suggested that the low activities of the analogues reflected a local perturbation of an essential contact between the analogue and its receptor. The side chain of ValB12 is located in a pocket consisting of residues B8−B11, B14−B17, B24, B26, and A13. Most of the pocket is filled up by the valine side chain, which may explain why smaller amino acids are preferred in this position when it comes to stabilizing the conformation of the molecule. Substitutions with amino acids that are too large may result in repulsive interactions either intramolecularly and thereby destabilize the conformation or intermolecularly and thereby destroy receptor–ligand interactions, whereas some of the favorable interactions will disappear if the amino acid becomes too small. The low expression yields obtained for the B12 library are suggestive of conformational changes that lower the folding stability of several of the analogue precursors, which is in agreement with earlier studies emphasizing the importance of the ValB12 residue in the overall structure of the hormone (*6, 57, 61*). Therefore, the severe reduction in binding affinity for some of the B12 analogues probably reflects long-range structural changes instead of a direct contribution of the altered amino acid side chain. However, the data obtained in this study together with results from other structural and mutational studies strongly support the belief that ValB12 is part of a receptor binding surface.

The tyrosine residue at B16 is situated in the proximity of ValB12 in the dimer-forming surface of insulin and is likewise suggested to be part of the classical binding surface. Cross-linking studies have shown that B16 maps to the L1 domain of the IR (*56*), and the results obtained in this study were strongly supportive of a direct interaction between TyrB16 and the IR. The amino acid scanning mutagenesis further revealed that the conservative aromatic amino acid substitutions to either Phe or Trp had no impact on IR binding, while the remainder of amino acid substitutions caused substantial reductions of up to 40-fold in binding affinities. The fact that analogues B16F and B16W both exhibit full binding affinity suggests that putative receptor interactions are of hydrophobic and possibly aromatic character rather than hydrogen bond dependent. Except for the B16A binding data, the results obtained from the amino acid scanning mutagenesis generally agreed with those obtained in previous studies (*62, 63*). The receptor binding activity of the B16A analogue was previously determined to be 69% compared to human insulin (*13*) and therefore not suggested to be part of the functional binding epitope. However, later investigations (*56, 59*), including this study, have found that the B16A analogue retains 27–34% of the receptor binding. Even though position B16 has less stringent spatial and stereochemical requirements for adequate receptor binding than B12, it appears that TyrB16 is indeed part of the insulin binding surface.

A small hydrophilic serine residue is normally residing in position B9 of the dimer-forming surface of insulin; however, large nonpolar aromatic amino acid substitutions were unexpectedly well accommodated at this position. The expression yields of analogue precursors B9F, B9W, and B9Y all exceeded that of the wild-type precursor, indicating proper folding and the relative binding affinities of the corresponding analogues were all similar to that of human insulin. The fact that both small hydrophilic and large hydrophobic amino acid substitutions at position B9 result in analogues showing almost fully retained binding affinities compared to that of human insulin suggested that SerB9 is not a part of insulin's binding surface.

Together, our results confirm the importance of residues ValB12 and TyrB16 in IR binding and also suggest that GluB13 is indeed part of a continual binding surface of insulin (see Figure 1c). Structural stabilization of the central helix and thereby a more rigid presentation of either side of the binding epitope at the IR surface seems to be important for receptor recognition, and it would therefore be of interest to perform circular dichroism (CD) experiments on a selection of analogues to support this proposition.

Without solution structures of the analogues in the monomeric state under physiologically relevant conditions, it is not possible to conclusively establish that the observed changes in receptor affinities are due to direct contributions of the altered side chains and not an induced conformational change in the binding epitope. However, with the exception of the B12 library, expression yields comparable to that of the wild-type precursor were obtained for the majority of the analogue precursors, indicating proper folding of the molecules. *S. cerevisiae* might also be unable to produce all the analogues in a given position, but regardless of these limitations, this method is a very powerful tool for identifying the structural requirements of the various positions of the insulin molecule essential for both insulin expression and IR binding.

In conclusion, we have developed a method for systematic amino acid scanning mutagenesis allowing us to confirm the importance of the B chain α-helix as a central recognition component in a continual binding surface. In combination with structural information as well as kinetic studies on a selection of the analogues, these data will provide valuable information about the mechanism of insulin binding.

ACKNOWLEDGMENT

Excellent technical assistance was provided by Annette Frost Pettersson, Lene Sloth Walander, Peter Riis Eriksen, Linda Kirk Nielsen, Gitte Norup, and Frantisek Hubálek. We thank Helle Naver for the purified insulin receptors and Lars Højlund Christensen for the fermentation of selected analogue strains.

REFERENCES

1. Derewenda, U., Derewenda, Z., Dodson, G. G., Hubbard, R. E., and Korber, F. (1989) Molecular structure of insulin, the insulin monomer and its assembly. *Br. Med. J. 45*, 4–18.
2. Seino, S., and Bell, G. I. (1989) Alternative splicing of human insulin receptor messenger RNA. *Biochem. Biophys. Res. Commun. 159*, 312–316.
3. Adams, M. J., Blundell, T. L., Dodson, E. J., Dodson, G. G., Vijayan, M., Baker, E. N., Harding, M. M., Hodgkin, D. C., Rimmer, B., and Sheat, S. (1969) Structure of rhombohedral 2 zinc insulin crystals. *Nature 224*, 491–495.
4. Blundell, T. L., Dodson, G., Hodgkin, D., and Mercola, D. (1972) Insulin: The structure in the crystal and its reflection in chemistry and biology. *Adv. Protein Chem. 26*, 279–402.
5. Kaarsholm, N. C., and Ludvigsen, S. (1995) The high resolution solution structure of the insulin monomer determined by NMR. *Receptor 5*, 1–8.
6. Baker, E. N., Blundell, T. L., Cutfield, J. F., Cutfield, S. M., Dodson, E. J., Dodson, G. G., Hodgkin, H. M., Hubbard, R. E., Isaacs, N. W., and Reynolds, C. D. (1988) The structure of 2Zn pig insulin crystals at 1.5 Å resolution. *Philos. Trans. R. Soc. London, Ser. B 19*, 369–456.
7. Marino-Buslje, C., Martin-Martinez, M., Mizuguchi, K., Siddle, K., and Blundell, T. L. (1999) The insulin receptor: From protein sequence to structure. *Biochem. Soc. Trans. 27*, 715–726.
8. Schaefer, E. M., Erickson, H. P., Federwisch, M., Wollmer, A., and Ellis, L. (1992) Structural organization of the human insulin receptor ectodomain. *J. Biol. Chem. 267*, 23393–23402.
9. Kjeldsen, T., Andersen, A. S., Wiberg, F. C., Rasmussen, J. S., Schäffer, L., Balschmidt, P., Møller, K. B., and Møller, N. P. H. (1991) The ligand specificities of the insulin receptor and the insulin-like growth factor I receptor reside in different regions of a common binding site. *Proc. Natl. Acad. Sci. U.S.A. 88*, 4404–4408.
10. McKern, N. M., Lawrence, M. C., Streltsov, V. A., Lou, M.-Z., Adams, T. E., Lovrecz, G. O., Elleman, T. C., Richards, K. M., Bentley, J. D., Pilling, P. A., Hoynem, P. A., Cartledge, K. A., Pham, T. M., Lewis, J. L., Sankovich, S. E., Stoichevska, V., Da Silva, E., Robinson, C. P., Frenkel, M. J., Sparrow, L. G., Fernley, R. T., Epa, V. C., and Ward, C. W. (2006) Structure of the insulin receptor ectodomain reveals a folded-over conformation. *Nature 443*, 218–221.
11. Conlon, J. M. (2001) Evolution of the insulin molecule: Insights into structure-activity and phylogenetic relationships. *Peptides 22*, 1183–1193.
12. Pullen, R. A., Lindsay, D. G., Wood, S. P., Tickle, I. J., Blundell, T. L., Wollmer, A., Krail, G., Brandenburg, D., Zahn, H., Gliemann, J., and Gammeltoft, S. (1976) Receptor-binding region of insulin. *Nature 259*, 369–373.
13. Kristensen, C., Kjeldsen, T., Wiberg, F. C., Schäffer, L., Hach, M., Havelund, S., Bass, J., Steiner, D. F., and Andersen, A. S. (1997) Alanine scanning mutagenesis of insulin. *J. Biol. Chem. 20*, 12978–12983.
14. Kitagawa, K., Ogawa, H., Burke, G. T., Chanley, J. D., and Katsoyannis, P. G. (1984) Critical role of the A2 amino acid residue in the biological activity of insulin: [2-glycine-A]- and [2-Alanine-A]insulins. *Biochemistry 23*, 1405–1413.
15. Nakagawa, S. H., and Tager, H. S. (1992) The importance of aliphatic side-chain structure at positions 2 and 3 of the insulin A chain in insulin-receptor interactions. *Biochemistry 31*, 3204–3214.
16. Xu, B., Hua, Q.-X., Nakagawa, S. H., Jia, W., Chu, Y.-C., Katsoyannis, P. G., and Weiss, M. A. (2002) Chiral mutagenesis of insulin's hidden receptor-binding surface: Structure of an allo-isoleucineA2 analogue. *J. Mol. Biol. 316*, 435–441.
17. Xu, B., Hu, S.-Q., Chu, Y.-C., Huang, K., Nakagawa, S. H., Whittaker, J., Katsoyannis, P. G., and Weiss, M. A. (2004) Diabetes-associated mutations in insulin: Consecutive residues in the B chain contact distinct domains of the insulin receptor. *Biochemistry 43*, 8356–8372.
18. Derewenda, U., Derewenda, Z., Dodson, E. J., Dodson, G. G., Bing, W., and Markussen, J. (1991) X-ray analysis of the single chain B29-A1 peptide-linked insulin molecule. A completely inactive analogue. *J. Mol. Biol. 220*, 425–433.
19. Hua, Q. X., Shoelsen, S. E., Kochoyan, M., and Weiss, M. A. (1991) Receptor binding redefined by a structural switch in a mutant human insulin. *Nature 354*, 238–241.
20. Nakagawa, S. H., and Tager, H. S. (1989) Pertubation of insulin-receptor interactions by intramolecular hormone cross-linking. *J. Biol. Chem. 264*, 272–279.
21. Ludvigsen, S., Olsen, H. B., and Kaarsholm, N. C. (1998) A structural switch in a mutant insulin exposes key residues for receptor binding. *J. Mol. Biol. 279*, 1–7.
22. Wan, Z.-L., Huang, K., Xu, B., Hu, S.-Q., Wang, S., Chu, Y.-C., Katsoyannis, P. G., and Weiss, M. A. (2005) Diabetes-associated mutations in human insulin: Crystal structure and photo-cross-linking studies of a A-chain variant insulin Wakayama. *Biochemistry 44*, 5000–5016.
23. Emdin, S. O., Sonne, O., and Gliemann, J. (1980) Hagfish insulin: The discrepancy between binding affinity and biologic activity. *Diabetes 29*, 301–303.
24. Emdin, S. O., Gammeltoft, S., and Gliemann, J. (1977) Degradation, receptor binding affinity, and potency of insulin from the Atlantic hagfish (*Myxine glutinosa*) determined in isolated rat fat cells. *J. Biol. Chem. 252*, 602–608.
25. Horuk, R., Blundell, T. L., Lazarus, N. R., Neville, R. W. J., Stone, D., and Wollmer, A. (1980) A monomeric insulin from the porcupine (*Hystrix cristata*), an Old World hystricomorph. *Nature 286*, 822–824.
26. Bajaj, M., Blundell, T. L., Horuk, R., Pitts, J. E., Wood, S. P., Gowan, L. K., Schwabe, C., Wollmer, A., Gliemann, J., and Gammeltoft, S. (1986) Primary structure, conformation and biological properties of a hystricomorph rodent insulin. *Biochem. J. 238*, 345–351.
27. Schäffer, L. (1994) A model for insulin binding to the insulin receptor. *Eur. J. Biochem. 221*, 1127–1132.
28. De Meyts, P. (1994) The structural basis of insulin and insulin-like growth factor-I receptor binding and negative co-operativity, and its relevance to mitogenic versus metabolic signalling. *Diabetologia 37*, S135–S148.
29. De Meyts, P., Roth, J., Neville, D. M., Gavin, J. R., and Lesniak, M. A. (1973) Insulin interactions with its receptors: Experimental evidence for negative cooperativity. *Biochem. Biophys. Res. Commun. 55*, 154–161.
30. Lou, M., Garret, T. P., McKern, N. M., Hoyne, P. A., Epa, V. C., Bentley, J. D., Lovrecz, G. O., Cosgrove, L. J., Frenkel, M. J., and Ward, C. W. (2006) The first three domains of the insulin receptor differ structurally from the insulin-like growth factor 1 receptor in the regions governing ligand specificity. *Proc. Natl. Acad. Sci. U.S.A. 103*, 12429–12434.
31. Ward, C. W., Lawrence, M. C., Streltsov, V. A., Adams, T. E., and McKern, N. M. (2007) The insulin and EGF receptor structures: New insights into ligand-induced receptor activation. *Trends Biochem. Sci. 32*, 129–137.
32. Kaarsholm, N. C., Norris, K., Jørgensen, R. J., Mikkelsen, J., Ludvigsen, S., Olsen, O. H., Sørensen, A. R., and Havelund, S. (1993) Engineering stability of the insulin monomer fold with application to structure-activity relationships. *Biochemistry 32*, 10773–10778.
33. Bentley, G. A., Brange, J., Derewenda, Z., Dodson, E. J., Dodson, G. G., Markussen, J., Wilkinson, A. J., Wollmer, A., and Xiao, B. (1992) Role of B13 Glu in insulin assembly. The hexamer structure of recombinant mutant (B13Glu→Gln) insulin. *J. Mol. Biol. 228*, 1163–1176.
34. Ludvigsen, S., Roy, M., Thøgersen, H., and Kaarsholm, N. C. (1994) High-resolution structure of an engineered biologically potent insulin monomer, B16Tyr→His, as determined by nuclear magnetic resonance spectroscopy. *Biochemistry 33*, 7998–8006.
35. Nakagawa, S. H., Tager, H. S., and Steiner, D. F. (2000) Mutational analysis of invariant valine B12 in insulin: Implications for receptor binding. *Biochemistry 39*, 15826–15835.
36. Soos, M. A., Siddle, K., Baron, M. D., Heward, J. M., Luzio, J. P., Bellantin, J., and Lennox, E. S. (1986) Monoclonal antibodies reacting with multiple epitopes on the human insulin receptor. *Biochem. J. 235*, 199–208.

37. Fujita-Yamaguchi, Y., Choi, S., Sakamoto, Y., and Itakura, K. (1983) Purification of insulin receptor with full binding activity. *J. Biol. Chem. 258*, 5045–5049.
38. Slaaby, R., Schäffer, L., Lautrup-Larsen, I., Andersen, A. S., Shaw, A. C., Mathiasen, I. S., and Brandt, J. (2006) Hybrid receptors formed by insulin receptor (IR) and insulin-like growth factor I receptor (IGF-IR) have low insulin and high IGF-1 affinity irrespective of the IR splice variant. *J. Biol. Chem. 281*, 25869–25874.
39. Kjeldsen, T., Pettersson, A. F., and Hach, M. (1999) The role of leaders in intracellular transport and secretion of the insulin precursor in the yeast *Saccharomyces cerevisiae*. *J. Biotechnol. 75*, 195–208.
40. Kjeldsen, T., Brandt, J., Andersen, A. S., Egel-Mitani, M., Hach, M., Pettersson, A. F., and Vad, K. (1996) A removable spacer peptide in an α-factor-leader/insulin precursor fusion protein improves processing and concomitant yield of the insulin precursor in *Saccharomyces cerevisiae*. *Gene 170*, 107–112.
41. Ho, S. N., Hunt, H. D., Horton, R. M., Pullen, J. K., and Pease, L. R. (1989) Site-directed mutagenesis by overlap extension using the polymerase chain reaction. *Gene 77*, 51–59.
42. Kjeldsen, T., Ludvigsen, S., Diers, I., Balschmidt, P., Sørensen, A. R., and Kaarsholm, N. C. (2002) Engineering-enhanced protein secretory expression in yeast with application to insulin. *J. Biol. Chem. 277*, 18245–18248.
43. Vølund, A. (1978) Application of the four-parameter logistic model to bioassay: Comparison with slope ratio and parallel line models. *Biometrics 34*, 357–365.
44. Kjeldsen, T., Balschmidt, P., Diers, I., Hach, M., Kaarsholm, N. C., and Ludvigsen, S. (2001) Expression of insulin in yeast: The importance of molecular adaptation for secretion and conversion. *Biotechnol. Genet. Eng. Rev. 18*, 89–121.
45. Schwartz, G. P., Burke, G. T., and Katsoyannis, P. G. (1987) A superactive insulin: [B10-aspartic acid]insulin(human). *Proc. Natl. Acad. Sci. U.S.A. 84*, 6408–6411.
46. De Meyts, P. (2004) Insulin and its receptor: Structure, function and evolution. *BioEssays 26*, 1351–1362.
47. Ma, J. C., and Dougherty, D. A. (1997) The cation-π interaction. *Chem. Rev. 97*, 1303–1324.
48. Crowley, P. B., and Golovin, A. (2005) Cation-π interactions in protein-protein interfaces. *Proteins 59*, 231–239.
49. Emdin, S. O., Dodson, G. G., Cutfield, J. M., and Cutfield, S. M. (1980) Role of zinc in insulin biosynthesis. *Diabetologia 19*, 174–182.
50. Carroll, R. J., Hammer, R. E., Chan, S. J., Swift, H. H., Rubenstein, A. H., and Steiner, D. F. (1988) A mutant human proinsulin is secreted from islets of Langerhans in increased amounts via an unregulated pathway. *Proc. Natl. Acad. Sci. U.S.A. 85*, 8943–8947.
51. Schwartz, G., Burke, G. T., and Katsoyannis, P. G. (1982) The importance of the B10 amino acid residue to the biological activity of insulin. [Lys10-B] human insulin. *J. Protein Chem. 1*, 177–189.
52. Burke, G. T., Schwartz, G., and Katsoyannis, P. G. (1984) Nature of the B10 amino acid residue. *Int. J. Pept. Protein Res. 23*, 394–401.
53. Richardson, J. S., and Richardson, D. C. (1988) Amino acid preferences for specific locations at the ends of α helices. *Science 240*, 1648–1652.
54. Aurora, R., and Rose, G. D. (1998) Helix capping. *Protein Sci. 7*, 21–38.
55. Chakrabartty, A., Doig, A. J., and Baldwin, R. L. (1993) Helix capping propensities in peptides parallel those in proteins. *Proc. Natl. Acad. Sci. U.S.A. 90*, 11332–11336.
56. Huang, K., Xu, B., Hu, S.-Q., Chu, Y.-C., Hua, Q.-X., Qu, Y., Li, B., Wang, S., Wang, R.-Y., Nakagawa, S. H., Theede, A. M., Whittaker, J., De Meyts, P., Katsoyannis, P. G., and Weiss, M. A. (2004) How insulin binds: The B-chain α-helix contacts the L1 β-helix of the insulin receptor. *J. Mol. Biol. 341*, 529–550.
57. Hu, S.-Q., Burke, G. T., Schwartz, G. P., Ferderigos, N., Ross, J. B. A., and Katsoyannis, P. G. (1993) Steric requirements at position B12 for high biological activity in insulin. *Biochemistry 32*, 2631–2635.
58. Brange, J., Ribel, U., Hansen, J. F., Dodson, G., Hansen, M. T., Havelund, S., Melberg, S. G., Norris, F., Norris, K., Snel, L., Sørensen, A. R., and Voigt, H. O. (1988) Monomeric insulins obtained by protein engineering and their medical implications. *Nature 333*, 679–682.
59. Chen, H., Shi, M., Gou, Z.-Y., Tang, Y.-H., Qiao, Z.-S., Liang, Z.-H., and Feng, Y.-M. (2000) Four new monomeric insulins obtained by alanine scanning the dimer-forming surface of the insulin molecule. *Protein Eng. 13*, 779–782.
60. Weiss, M. A., Hua, Q.-X., Lynch, C. S., Frank, B. H., and Shoelson, S. E. (1991) Heteronuclear 2D NMR studies of an engineered insulin monomer: Assignment and characterization of the receptor-binding surface by selective ^{2}H and ^{13}C labelling with application to protein design. *Biochemistry 30*, 7373–7389.
61. Gou, Z.-Y., Wang, S., Tang, Y.-H., and Feng, Y.-M. (2004) Mutagenesis of the three conserved valine residues: Consequence on the foldability of insulin. *Biochim. Biophys. Acta 1699*, 103–109.
62. Hu, S.-Q., Burke, G. T., and Katsoyannis, P. G. (1993) Contribution of the B16 and B26 tyrosine residues to the biological activity of insulin. *J. Protein Chem. 12*, 741–747.
63. Schwartz, G. P., Wong, D., Burke, G. T., de Vroede, M. A., Rechler, M. M., and Katsoyannis, P. G. (1985) Glutamine B16 insulin: Reduced insulin-like metabolic activity with moderately preserved mitogenic activity. *J. Protein Chem. 4*, 185–197.
64. Smith, G. D., Pangborn, W. A., and Blessing, R. H. (2003) The structure of T6 human insulin at 1 Å resolution. *Acta Crystallogr. D59*, 474–482.
65. De Lano, W. L. 2002 The PyMOL Molecular Graphics System, DeLano Scientific, San Carlos, CA.

BI800054Z